

## On the Robustness of Low-frequency Laser Control Schemes for Proton Transfer in Thioacetylacetone\*

Iva Tatić<sup>a</sup> and Nađa Došlić<sup>b,\*\*</sup>

<sup>a</sup>Department of Chemistry, Faculty of Science, University of Zagreb, Marulićev trg 19, 10000 Zagreb, Croatia

<sup>b</sup>Department of Physical Chemistry, Ruđer Bošković Institute, Bijenička 54, 10000 Zagreb, Croatia

RECEIVED FEBRUARY 14, 2003; REVISED JUNE 6, 2003; ACCEPTED JUNE 9, 2003

The paper investigates quantum control of the proton transfer reaction in a two-dimensional model system using terahertz (THz) laser fields. The model potential, tailored to MP2 data for thioacetylacetone, comprises the proton transfer and the heavy atom coordinates. Two distinct mechanisms of proton transfer are investigated: the resonant *versus* the tunneling one. The efficiency of laser control in both cases is tested against the instability of pulse characteristics. The study shows that while the resonant scheme allows efficient control for a large range of field parameters, the tunneling scheme is very sensitive to the pulse characteristics, and therefore experimentally hardly realizable.

*Key words*  
low-frequency laser  
proton transfer  
thioacetylacetone

### INTRODUCTION

There is no doubt that ultrafast laser spectroscopy has deeply influenced research in different areas of modern chemistry and biology.<sup>1–3</sup> In particular, the issue of laser control of chemical reactions has received considerable attention in the last decade.<sup>4</sup> Here, detailed understanding of both the laser-matter interaction and relaxation processes occurring in the molecules is required to take full advantage of the possibilities offered by the up-to-date ultrafast equipment. Recent advances in generation of THz laser pulses<sup>5</sup> enabled experimental studies of quantum transport phenomena<sup>6,7</sup> and opened the possibility of manipulating these effects for controlling molecular dynamics.

Here we theoretically explored the possibility of controlling the proton transfer dynamics in asymmetric molecular systems by using picosecond THz laser pulses.<sup>8–10</sup>

Two laser control mechanisms emerged from these studies. In the resonant scheme, the laser frequency matches the energy difference between the two lowest states in the system (localized in the reactant and product wells), and by exploiting the non-zero dipole momentum between them induces a population switch in the molecule. The second mechanism, most easily understandable in the so-called dressed molecular state representation, is based on the idea of perturbing the system potential in such a way that the initial asymmetry in the molecular potential is removed. The lowest eigenstates of the system are then brought into resonance for a time needed for the proton to tunnel from the reactant to the product well of the system. Although the underlying mechanisms are rather different, it has been shown that both schemes perform equally well in dissipative and non-dissipative environments.<sup>9,10</sup> Also, both schemes require a similar

\* Dedicated to Professor Nenad Trinajstić on the occasion of his 65<sup>th</sup> birthday.

\*\* Author to whom correspondence should be addressed. (E-mail: nadja.doslic@irb.hr)

field intensity and picosecond pulse duration. Neither of these works was focused on the robustness of the proposed schemes, *i.e.*, on the feasibility of their experimental realization. Here, we will explore the efficiency of the two schemes with respect to changes in the laser frequency and/or field intensities. For this purpose we will use a two-dimensional model Hamiltonian tailored to thioacetylacetone, a molecule for which a large body of experimental and theoretical results is available.<sup>8,9,12-14</sup>

## THE MODEL HAMILTONIAN

It is well known that accurate calculation of the proton potential in H-bonded systems requires inclusion of dynamical correlation effects. This can be most easily achieved by using the second order Møller-Plesset perturbation theory (MP2)<sup>15</sup> or by employing the computationally less expensive Density Functional Theory (DFT),<sup>16</sup> while the more sophisticated CCSD(T) method is computationally quite expensive. It has been emphasized in a number of studies on hydrogen bonded systems that due to overestimation of correlation effects, DFT gives too low energy barriers for proton transfer. Recently, it has been shown<sup>17</sup> that the B1LYP functional could be an adequate choice for potential energy surface calculations in such systems. For the molecule at hand, thioacetylacetone, the B1LYP/6-311++G\*\* method gives a proton transfer (PT) energy barrier of 5.2 kcal mol<sup>-1</sup>, which is in good agreement with the MP2 barrier of 5.3 kcal mol<sup>-1</sup>.<sup>14</sup> It is noteworthy that like in acetylacetone<sup>18-25</sup> the proton transfer in TAA is coupled with rotation of the two methyl groups.

In this work we have employed a two-dimensional potential energy surface adapted from MP2(full)/6-31+

G(d,p) calculations. The model potential, which comprises the proton transfer coordinate ( $x$ ) and the heavy atom coordinate ( $Q$ ), is discussed in detail in Refs. 8,9. The potential along the PT coordinate is obtained by fitting quantum chemical data, and can be expressed as

$$V_x(x) = \frac{1}{2} [V_{\text{osc}}^{(1)}(x) + V_{\text{osc}}^{(2)}(x) - \sqrt{(V_{\text{osc}}^{(1)}(x) - V_{\text{osc}}^{(2)}(x))^2 + 4K^2(x)}] \quad (1)$$

The potential has been obtained using two shifted ( $\Delta_i$ ) harmonic functions  $V_{\text{osc}}^{(i)}(x) = k_i (x-x_{0,i})^2 / 2 + \Delta_i$  coupled by a Gaussian function  $K(x) = k_c \exp\{-(x-x_c)^2\}$  with amplitude  $k_c$ . Index  $i = 1,2$  refers to the enol and enethiol forms, respectively. All parameters of the potential are listed in Refs. 8,9.

The potential for the heavy atom motion can be modeled by a function of the form<sup>8,9</sup>

$$V_Q(x,Q) = \frac{k_Q}{2} (Q - f(x))^2 \quad (2)$$

where the asymmetry of the TAA potential is taken into account through the coupling function  $f(x) = ax^2 + bx^3$ . The molecular Hamiltonian therefore reads:

$$H_0 = \frac{P_x^2}{2\mu_x} + \frac{P_Q^2}{2\mu_Q} + V_x(x) + V_Q(x,Q) \quad (3)$$

Here,  $\mu_x = 1.05$  u and  $\mu_Q = 4.73$  u are the reduced masses for the motion along the PT and the heavy atom coordinate, respectively.

The time independent Schrödinger equation  $H_0 \phi_i(x,Q) = E_v \phi_v(x,Q)$  has been solved using the Fourier grid Hamiltonian method.<sup>26</sup> The two lowest eigenfunctions  $\phi_0$  and  $\phi_1$ , corresponding to the enol and enethiol forms of TAA are

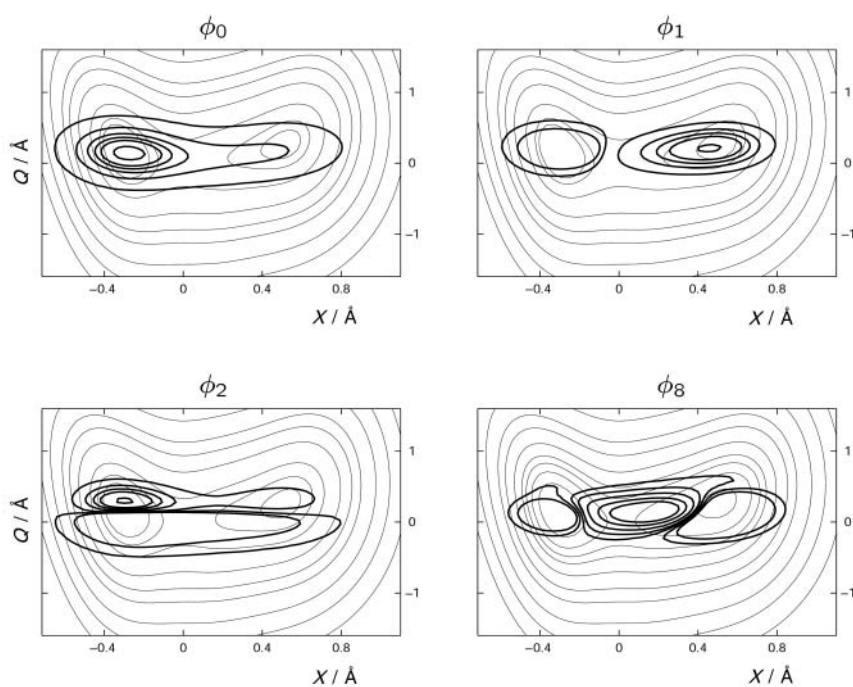


Figure 1. The two-dimensional potential energy surface (isolines at 0.1, 0.2, 0.3, 0.4, 0.6, 0.9, 1.2, 1.8, 2.5 eV) is shown together with the density plots of vibrational eigenstates (from left to right and top to bottom)  $\phi_0$ ,  $\phi_1$ ,  $\phi_2$ ,  $\phi_8$ .

shown in Figure 1 together with the model potential. The first excited state in heavy atom coordinate  $\phi_2$  and the first excited state in the PT direction  $\phi_8$  are shown as well.

In order to investigate the laser driven proton dynamics, one has to define the Hamiltonian of the interaction between the molecule and the electromagnetic field. In the dipole approximation, the interaction Hamiltonian is given by

$$H_F(t) = -d(x, Q) E(t) \quad (4)$$

where  $d(x, Q)$  is the dipole moment (for details see Refs. 8,9) and  $E(t)$  is the Gaussian shaped laser field

$$E(t) = E_0 \left( \frac{2}{\Delta^2 \pi} \right)^{1/2} e^{-2(t-t_0)^2/\Delta^2} \cos(\omega t) \quad (5)$$

with amplitude  $E_0$ , carrier frequency  $\omega$ , duration  $t_0$ , and width  $\Delta$ . The total Hamiltonian is then given by  $H = H_0 + H_F$ .

The solution of the time dependent Schrödinger equation

$$i\hbar \frac{d\psi}{dt} = H\psi \quad (6)$$

has been obtained by expansion of  $\psi(x, Q, t)$  in the basis of the system eigenfunctions  $\varphi_v(x, Q)$

$$\psi(x, Q, t) = \sum_v a_v(t) \varphi_v(x, Q) \quad (7)$$

The coefficients  $a_v(t)$  are then determined by solving the set of coupled first-order differential equations:

$$i\hbar \frac{da_v}{dt} = a_v E_v - E(t) \sum_{\mu} \langle v | d(x, Q) | \mu \rangle a_{\mu}(t) \quad (8)$$

The numerical solution of Eq. (8) was obtained using the standard fourth-order Runge-Kutta method. In order to take account of possible multiphoton transitions, fifteen eigenstates were included into the calculation. In the following, the dynamics of the system will be monitored by the population of each state given by:

$$P_v(t) = |a_v(t)|^2 \quad (9)$$

## RESULTS AND DISCUSSION

From spectroscopic data it is known that  $\beta$ -thioxoketones exist as a mixture of interconverting enol and enethiol forms. As this work aims to compare the efficiency and robustness of the two laser control schemes for enol-enethiol interconversion, we consider the system in the enol form. The first excited vibrational state (enethiol form) has been chosen as the target state.

### The Resonant Scheme

Within the resonant scheme, the field parameters for an efficient population inversion are obtained from the

so-called  $\pi$ -pulse criteria. We know from the two-level systems theory<sup>27</sup> that the transition amplitude is a function of the pulse area defined by

$$\sigma(t) = d_{01} / \hbar \int_0^t s(t') dt' \quad (10)$$

where  $d_{01} = \langle \phi_0 | d(x, Q) | \phi_1 \rangle$  is the transition dipole moment, and  $s(t)$  is the slowly varying field amplitude. When the time integral of the Rabi frequency (the pulse area) is equal to  $\pi$ , a complete population inversion occurs between the two states. Tuning the pulse frequency into resonance with the  $\phi_0 \rightarrow \phi_1$  transition and following the  $\pi$ -pulse criteria, we found that the laser pulse shown in Figure 2a, with parameters  $\varepsilon_0 = 0.0103$  u,  $\omega = 8.12 \times 10^{-4}$  u ( $178.2 \text{ cm}^{-1}$ ) and duration  $t_0 = 1300$  fs, induces an almost complete population switch in the system.<sup>9</sup> The underlying state dynamics can be conveniently monitored by calculating the instantaneous eigenvalues of the time-dependent Hamiltonian<sup>28</sup>

$$(H_0 - \varepsilon(t)d) \phi_n^{\varepsilon} = E_n^{\varepsilon} \phi_n^{\varepsilon} \quad (11)$$

In Figure 2b, we plot the field dependence of the eigenenergies  $E_n^{\varepsilon}$  for the six lowest states. First, we notice that the interaction with the laser field causes mix-

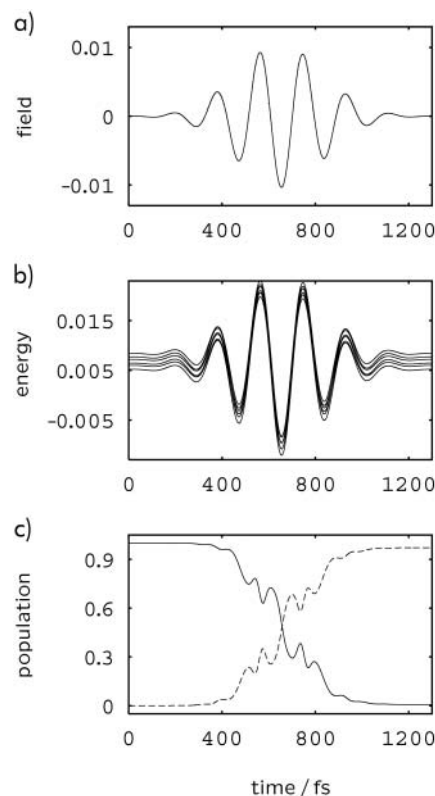


Figure 2. The laser field for the resonant approach to the laser driven proton transfer is presented in the upper panel. The field dependence of the eigenenergies  $E_n^{\varepsilon}$  for the six lowest states of TAA (middle panel) and the population dynamics of the two lowest eigenstates during the isomerization reaction (lower panel). The laser field and energies are given in atomic units.

ing of instantaneous eigenvalues in the system. Due to the resonant laser field, all states of the system experience a strong optical Stark effect (or ac Stark effect),<sup>29</sup> and the effect is most pronounced in the two lowest eigenvalues. This gives rise to an efficient population transfer between the two lowest states, as shown in Figure 2c. It can be observed that the time-dependence of the population transfer rates follows the oscillatory pattern of the field dressed eigenvalues.

### The Tunneling Scheme

Next, we explore the efficiency of the tunneling scheme. The amplitude of the tunneling pulse  $\varepsilon_0$  can be calculated from the matrix elements of the Hamiltonian Eq. (12) and is given by<sup>30</sup>

$$\varepsilon_0 = \frac{E_1 - E_2}{d_{00} - d_{11}} \quad (12)$$

where  $E_0$  and  $E_1$  are eigenvalues of the ground and first excited states. A plateau type pulse<sup>8</sup> with amplitude  $\varepsilon_0$  given by Eq. (12) induces a complete population transfer between the reactant and the product within the tunneling time  $\tau = h/4\pi\varepsilon_0 d_{01}$ . Note that in TAA, in order to compensate for the positive value of  $d_{00} - d_{11}$ , the tunneling field has a negative amplitude  $\varepsilon_0$ .

Here, we consider an almost half-cycled pulse with parameters  $\varepsilon_0 = -0.009848$  u,  $\omega = 3.9 \times 10^{-5}$  u ( $8.7 \text{ cm}^{-1}$ ) and duration  $t_0 = 1200$  fs, which is shown in the upper panel of Figure 3. This type of pulse, experimentally realizable in the femtosecond time domain, can be considered as a limiting case of the plateau type pulse<sup>8</sup> with zero duration of the plateau period. The instantaneous eigenvalues for the tunneling pulse and the correspondent population dynamics are plotted in the middle and lower panels of Figure 3. The pulse initially creates a superposition of two delocalized states which are eigenstates of the molecule dressed by the laser field, Eq. (11). In the following stage when the two lowest instantaneous eigenvalues are very close to each other, the dynamics proceeds by tunneling. At the end of the pulse the field is switched off, and the wave function is stabilized in the target state. While the resonant pulse brings a number of eigenvalues close to each other, the tunneling pulse is more selective, and only the two closest eigenvalues become near degenerate. The population dynamics of the two lowest zeroth-order states is shown in the lower panel of Figure 3. Like in the case of the resonant pulse, the tunneling pulse induces an almost complete population switch in the system.

### Isomerization Efficiency

Let us now consider the efficiency of the isomerization against the instability of the pulse characteristics. In Figure 4, we plotted the dependence of the occupation probability  $P_1$  of the target state on the amplitude and the frequency of the laser pulses. The laser field amplitude was

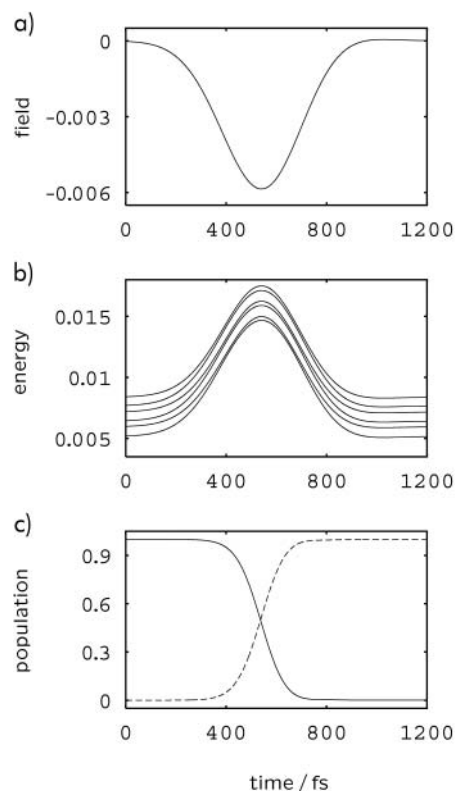


Figure 3. The laser field for the tunneling approach to isomerization is shown in the upper panel. The field dependence of the eigenenergies  $E_n^\varepsilon$  for the six lowest states of TAA (middle panel). The population dynamics of the two lowest eigenstates is shown in the lower panel. The laser field and energies are given in atomic units.

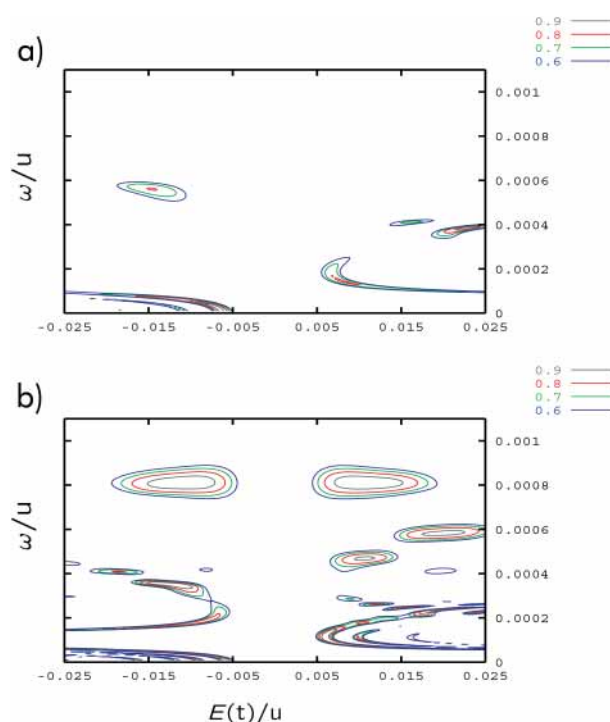


Figure 4. The population of the target  $\phi_1$  state against the instability of the pulse characteristics (pulse intensity and frequency) for laser pulse duration of  $t_0 = 800$  fs (upper panel), and  $t_0 = 1300$  fs (lower panel).



varied in a uniform way between  $-0.025 \leq \varepsilon_0 \leq 0.025$  u with an increment of  $\Delta \varepsilon_0 = 0.0005$  u while the laser frequency was varied between  $0 \leq \omega \leq 0.00112$  u ( $245.8 \text{ cm}^{-1}$ ) with an increment of  $\Delta \omega = 3.75 \times 10^{-6}$  u ( $0.8 \text{ cm}^{-1}$ ). The duration of the laser pulses was fixed at  $t_0 = 800$  fs (upper panel) and  $t_0 = 1300$  fs (lower panel). From Figure 4a it is evident that for the subpicosecond pulse duration, an appreciable population transfer occurs only in the low frequency region, *i.e.*, the proton transfer proceeds by laser driven tunneling. The range of parameters for which an efficient population transfer is achieved ( $P_1 \geq 0.8$ ) is very restricted. The reduction and fragmentation of the high yield areas is due to the fact that non-optimal pulses get the instantaneous eigenstates close to each other for a period shorter than the required tunneling time. On the other hand, for longer pulses ( $t_0 = 1300$  fs, Figure 4b), the reaction yield is higher than  $P_1 = 0.8$  (red) for a range of parameters in the resonant region satisfying only approximately the  $\pi$ -pulse condition. The shape of the resonant pulse allows efficient laser control for positive as well as for negative values of the laser field amplitude. It is also noteworthy that two areas of control with reaction yields higher than  $P_1 = 0.8$  appear for  $\varepsilon = 0.01$  u,  $\omega = 0.00048$  u ( $105 \text{ cm}^{-1}$ ) and for  $\varepsilon = 0.02$  u,  $\omega = 0.00058$  u ( $127 \text{ cm}^{-1}$ ). Unlike in the resonant case, no appreciable control was achieved in the mirror areas (positive field amplitudes). The changes induced by the two pulses on the instantaneous eigenvalues indicate that the underlying mechanism is a combination of the resonant and tunneling schemes. The most striking feature of Figure 4, however, is the fragmentation of the controllability areas below  $\omega = 2.4 \times 10^{-6}$  a. u. ( $55 \text{ cm}^{-1}$ ). Like in the previous case, no appreciable control could be achieved outside very restricted amplitude and frequency areas.

Finally, the instability of the laser driven isomerization in the tunneling regime has a direct implication on the possible experimental realization of the scheme. From the point of view of the required pulse intensities, both schemes appear feasible for experimental realization. However, the extreme sensitivity of the tunneling scheme under initial conditions makes the resonant scheme more appropriate for actual experiments.

## CONCLUSION

We have investigated the robustness of two laser control schemes for isomerization in proton transfer systems. Numerical simulation was performed using a two-dimensional model potential describing the proton transfer reaction in thioacetylacetone. On the basis of the solutions of the time-dependent Schrödinger equation, we found that the resonant scheme as well as the tunneling one induce an efficient proton switch in the molecule. The underlying dynamics was monitored by calculating the instantaneous eigenvalues of the time-dependent Hamiltonian. We have

shown that, within the resonant scheme, population inversion can occur for quite a wide range of laser field parameters. On the other hand, the tunneling scheme has proven to be very sensitive to changes in pulse parameters. No appreciable control could be achieved outside very restricted parameter area. This makes the tunneling scheme less suitable for experimental application.

*Acknowledgements.* – We thank Dr. O. Kühn for his contribution to developing the model potential for TAA. This work has been supported by the Ministry of Science and Technology of the Republic of Croatia, Project No. 06MP033.

## REFERENCES

1. J. Takeda, D. D. Chung, J. Zhou, and K. A. Nelson, *Chem. Phys. Lett.* **290** (1998) 341–348.
2. J. T. Fourkas, *Annu. Rev. Phys. Chem.* **53** (2002) 17–40.
3. L. Yoder, A. Cole, and R. Sension, *Photosynth. Res.* **72** (2002) 147–158.
4. J. Manz in: V. Sundström (Ed.), *Femtochemistry and Femtobiology*, Imperial College Press, London, 1997, p. 80.
5. L. Friedman, G. Sun, and R. A. Soref, *Appl. Phys. Lett.* **78** (2001) 401–403.
6. D. S. Citrin, *Phys. Rev. B* **60** (1999) 5659–5663.
7. A. Wacker, *Phys. Rep.* **357** (2002) 1–111.
8. N. Došlić, K. Sunderman, L. Gonzales, O. Mo, J. Giraud-Girard, and O. Kühn, *Phys. Chem. Chem. Phys.* **1** (1999) 1249–1257.
9. N. Došlić and O. Kühn, *Chem. Phys.* **255** (2000) 247–257.
10. V. May and O. Kühn, *Charge and Energy Transfer Dynamics in Molecular Systems*, Wiley-VCH, Berlin, 2000.
11. N. Došlić, J. Mavri, and J. Stare, *Chem. Phys.* **269** (2001) 59–73.
12. B. Andersen, F. Duus, S. Bolvig, and P. E. Hansen, *J. Mol. Struct.* **552** (2000) 45–62.
13. Y. Posokhov, A. Gorski, J. Spanget-Larsen, F. Duus, P. E. Hansen, and J. Waluk, *Chem. Phys. Lett.* **350** (2001) 502–508.
14. G. Fischer and J. Fabian, *Z. Phys. Chemie* **209** (1999) 75–92.
15. S. Sekušak and A. Sabljic, *Chem. Phys. Lett.* **272** (1997) 353–360.
16. N. Došlić, D. Babić, and S. D. Bosanac, *Chem. Phys. Lett.* **358** (2002) 337–343.
17. C. Adamo and V. Barone, *Chem. Phys. Lett.* **274** (1997) 242–250.
18. M. Johnson, N. Jones, A. Geis, A. Horsewill, and H. Trommsdorff, *J. Chem. Phys.* **116** (2002) 5694–5700.
19. J. Mavri and J. Grdadolnik, *J. Phys. Chem. A* **105** (2001) 2039–2044.
20. J. Mavri and J. Grdadolnik, *J. Phys. Chem. A* **105** (2001) 2045–2051.
21. O. A. Sharafeddin, K. Hinsin, T. Carrington, and B. Roux, *J. Comput. Chem.* **18** (1997) 1760–1772.
22. K. Wolf, W. Mikenda, E. Nusterer, and K. Schwarz, *J. Mol. Struct.* **448** (1989) 201–207.
23. K. Hinsin and B. Roux, *J. Comput. Chem.* **18** (1997) 368–380.
24. K. Hinsin and B. Roux, *J. Chem. Phys.* **106** (1997) 3567–3577.

25. M. E. Tuckerman and D. Marx, *Phys. Rev. Lett.* **86** (2001) 4946–4949.
26. C. C. Marston and G. Balint-Kurti, *J. Chem. Phys.* **91** (1989) 3571–3576.
27. L. Allen and J. H. Eberly, *Optical Resonance and Two-level Atoms*, Dover, New York, 1987.
28. O. Kühn, Y. Zhao, F. Shuang, and Y. Yan, *J. Chem. Phys.* **112** (2000) 6104–6112.
29. S. Mukamel, *Principles of Nonlinear Optical Spectroscopy*, Oxford University Press, New York, 1995.
30. H. Naundorf, K. Sundermann, and O. Kühn, *Chem. Phys.* **240** (1998) 163–172.

---

## SAŽETAK

### O postojanosti nisko frekventnih shema laserskog upravljanja prijenosom protona u tioacetilacetonu

Iva Tatić i Nađa Došlić

Istraživana je laserska kontrola prijenosa protona u dvodimenzionalnom modelnom sustavu rabeći terahertzne (THz) laserske pulseve. Modelni potencijal, dobiven na temelju MP2 podataka za tioacetilaceton, sastoji se od koordinate koja opisuje prijenos protona i koordinate gibanja teških atoma. Istražena su dva mehanizma laserske kontrole: rezonantni i tunelirajući. Posebna pozornost posvećena je osjetljivosti na nestabilnost laserskog pulsa. Dok je rezonantna shema učinkovita u širokom frekvencijskom području, tunelirajuća se shema pokazala vrlo osjetljivom na promjene frekvencije i inteziteta laserskog polja te stoga eksperimentalno manje pogodnom.